Investigation of time-integration and iterative techniques for nonequilibrium phosphorus diffusion modeling

Anand L. Pardhanani and Graham F. Carey
CFD Laboratory, WRW 301, The University of Texas, Austin, Texas 78712.

***Abstract*—We investigate numerical integration and iterative solution strategies for a class of reaction-diffusion systems used for modeling nonequilibrium phosphorus diffusion in silicon. These problems typically yield stiff systems of equations, and their efficient numerical simulation requires the use of stable integration strategies along with fast, robust algebraic system solvers. We compare the numerical performance of semi-implicit Runge-Kutta methods in conjunction with several standard nonsymmetric iterative solvers and multigrid methods.**

I. Introduction

The use of stiffly-stable integration methods and iterative solution strategies has proven effective in many reaction-diffusion applications. Such schemes also appear promising for the phosphorus diffusion models that we consider here. Various implicit integration techniques have been investigated in the literature for these problems including, for instance, the trapezoidal rule and its variants [1], backward difference formulas [2] and Adams-Moulton predictor-corrector schemes [3]. In this work we consider the semi-implicit Runge-Kutta methods which are known for their excellent stability properties. They have not been widely used in the past since they lead to multiple linear algebraic systems which must be solved at each integration step. This is where iterative and multigrid methods must be employed to efficiently solve the algebraic systems. The present work explores several generalized gradient type iterative schemes that are designed for nonsymmetric and/or indefinite algebraic systems. We also consider different smoothing approaches in multigrid algorithms in an effort to improve their robustness.

II. Phosphorus Diffusion Model

In our numerical studies we consider the 5-species phosphorus diffusion model by Richardson and Mulvaney [2], [3], which can be written as the following system of reaction-diffusion equations

$$\begin{aligned}
\frac{\partial V}{\partial t} &= D_V\nabla^2 V - k^E_{\text{for}}PV + k^E_{\text{rev}}E - k_{\text{bi}}(VI - V^{\text{eq}}I^{\text{eq}}) \\
\frac{\partial I}{\partial t} &= D_I\nabla^2 I - k^F_{\text{for}}PI + k^F_{\text{rev}}F - k_{\text{bi}}(VI - V^{\text{eq}}I^{\text{eq}}) \\
\frac{\partial E}{\partial t} &= D_E\nabla^2 E + k^E_{\text{for}}PV - k^E_{\text{rev}}E \qquad (1)\\
\frac{\partial F}{\partial t} &= D_F\nabla^2 F + k^F_{\text{for}}PI - k^F_{\text{rev}}F \\
\frac{\partial P}{\partial t} &= -k^E_{\text{for}}PV + k^E_{\text{rev}}E - k^F_{\text{for}}PI + k^F_{\text{rev}}F
\end{aligned}$$

where the solution vector $\boldsymbol{u} = [V, I, E, F, P]^T$ represents, respectively, the concentration of vacancies, interstitials, phosphorus-vacancy pairs (E-centers), phosphorus-interstitial pairs and substitutional phosphorus atoms.The diffusivities and reaction rates are constant, and their numerical values at 900°C temperature are estimated in [2], [3] as

$$\begin{aligned}
&D_V = 10^{-10},\ D_I = 10^{-9},\ D_E = 10^{-13}, \\
&D_F = 2\times 10^{-13}[\text{all } D\text{'s in units of cm}^2s^{-1}] \\
&k^E_{\text{for}} = k^F_{\text{for}} = 10^{-14}\ \text{cm}^3s^{-1}, \qquad (2)\\
&k^E_{\text{rev}} = 10s^{-1},\ k^F_{\text{rev}} = 12s^{-1}\ \ k_{\text{bi}} = 10^{-10}\ \text{cm}^3s^{-1}, \\
&V^{\text{eq}} = I^{\text{eq}} = 10^{14}\ \text{cm}^{-3}
\end{aligned}$$

For all species zero-flux boundary conditions are enforced everywhere except at the exposed surfaces, where we specify V, I, E, F and P as

$$V = V^{\text{eq}},\ \ I = I^{\text{eq}},\ \ E = \frac{k^E_{\text{for}}}{k^E_{\text{rev}}}PV,\ \ F = \frac{k^F_{\text{for}}}{k^F_{\text{rev}}}PI$$
$$P = C^* \text{ (ambient gas concentration)},$$

III. Numerical Formulation

The PDE system is discretized using the method of lines, and the resulting ODE system is integrated in fully-coupled, implicit form using either a backward Euler scheme or semi-implicit Runge-Kutta methods. The discretization is performed using a 9-point mapped finite difference strategy for nonuniform, structured grids. We consider 2nd and 3rd order integration schemes with 2 and 3 stages respectively. For an ODE system of the form $\frac{d\boldsymbol{u}}{dt} = \boldsymbol{F}(\boldsymbol{u})$, these schemes can be written in the following general form [4]

$$\boldsymbol{u}^{n+1} = \boldsymbol{u}^n + \Delta t\sum_{i=1}^{q}\alpha_i\boldsymbol{k}_i \qquad (3)$$

A. L. Pardhanani, 512-471-4069, anand@cfdlab.ae.utexas.edu.
G. F. Carey, 512-471-4207, carey@cfdlab.ae.utexas.edu.
This work is supported in part by DARPA contract # DABT 63-96-C-0067 and by the Texas Advanced Technology Program.

0-7803-3775-1/97/$10.00 © 1997 IEEE.

where q denotes the number of stages, and $\boldsymbol{k}_i$ has the form

$$\boldsymbol{k}_i = [\boldsymbol{F}(\boldsymbol{u}^n + \Delta t \sum_{j=1}^{i-1} b_j \boldsymbol{k}_j) + \Delta t\, a_i \boldsymbol{A}(\boldsymbol{u}^n + \Delta t \sum_{j=1}^{i-1} c_j \boldsymbol{k}_j)\, \boldsymbol{k}_i] \quad (4)$$

Here $\boldsymbol{A}$ is the Jacobian matrix of $\boldsymbol{F}$ with respect to $\boldsymbol{u}$, and the α_i, a_i, b_j and c_j are constants that depend upon the specific integration scheme under consideration. Note that each stage involves a function/Jacobian evaluation and linear system solution.

The linear systems are solved using either direct/band elimination or one of a suite of iterative methods in the parallel PCG package [5]. These include a variety of generalized gradient iterative schemes such as biconjugate gradient (BCG), BCG squared (CGS), CGS with stabilization (CGSTAB), QMR and GMRES. We also explore multigrid schemes for iteratively solving these systems. Designing effective iterative or multigrid schemes for this class of problems is challenging since the resulting linear systems are strongly nonsymmetric and far from diagonal-dominance. In particular, the PDE's for E and F in (1) with the coefficient values given in (2) contribute large off-diagonal entries in the Jacobian matrix of the discretized system. For example, if we discretize the PDE for E in 1D assuming a 1 micron domain-length with 100 uniform mesh cells, the diagonal entry in the Jacobian matrix is of the order $-D_V/h^2 - k^E_{\text{rev}} \sim 10$ (s^{-1}). On the other hand, the off-diagonal entries corresponding to the derivatives with respect to V and P are respectively of order $k^E_{\text{for}} P$ and $k^E_{\text{for}} V$. The value of P near the exposed surface is close to the concentration of phosphorus in the ambient gas which, in our test cases, is $\sim 10^{21}$ cm^{-3}. Thus, there are some rows in the Jacobian matrix where this off-diagonal entry is $\sim 10^7$, while the diagonal entry is ~ 10. This severely degrades the performance and robustness of iterative methods.

We have investigated multigrid algorithms with a few different variations in the smoothing strategy. The basic idea in multigrid methods is to use a sequence of nested grids in the discretization, and to iteratively solve the original problem by accumulating corrections from the nested sub-grids [6]. A key component of multigrid algorithms is an iterative relaxation process that is used for locally smoothing the errors at each grid level. Effectiveness of the smoothing mechanism in damping oscillatory components of the error is critical to the success of the multigrid algorithm.

In the present work we have explored variations of Gauss-Seidel relaxation, which is very commonly used in multigrid schemes. The PDE is discretized and the Jacobian matrix assembled in 5×5 blocks for the 5 unknowns at each grid node; i.e., it has the form

$$\boldsymbol{A} = \begin{bmatrix} \boldsymbol{A}_{11} & \boldsymbol{A}_{12} & \boldsymbol{A}_{13} & \cdots & \boldsymbol{A}_{1N} \\ \boldsymbol{A}_{21} & \boldsymbol{A}_{22} & \boldsymbol{A}_{23} & \cdots & \boldsymbol{A}_{2N} \\ \vdots & & & & \\ \boldsymbol{A}_{N1} & \boldsymbol{A}_{N2} & \boldsymbol{A}_{N3} & \cdots & \boldsymbol{A}_{NN} \end{bmatrix} \quad (5)$$

where each $\boldsymbol{A}_{ij}$ is a 5×5 matrix and N is the total number of grid nodes. The 9-point stencil, of course, implies that all except 9 of the submatrices in each row of $\boldsymbol{A}$ are zero. In the multigrid algorithm, we consider both point and line relaxation forms of the Gauss-Seidel scheme, with the provision that all the unknowns at each grid point or line be solved simultaneously. This is often referred to as "collective" point or line Gauss-Seidel smoothing in the multigrid literature. We have implemented 3 variants of this scheme: (1) collective point Gauss-Seidel, (2) collective line Gauss-Seidel with sweeps in either x- or y-direction, and (3) collective line Gauss-Seidel with alternating sweeps in both directions. Each variant exhibits somewhat different smoothing properties as we shall see in the results.

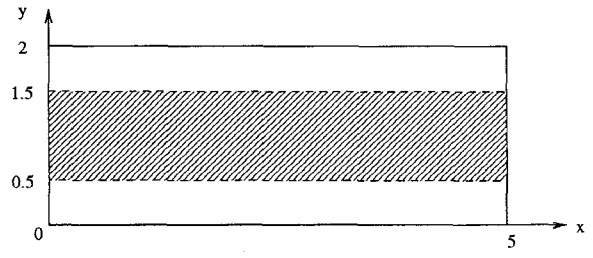

Fig. 1. Geometry and dimensions of domain used in test cases; shaded area along $x = 0$ represents exposed area in 2D test.

IV. Results and Discussion

Numerical simulations for the 5-species model (1) have been carried out in one- and two-dimensions at 900°C for the predeposition test case considered by Richardson and Mulvaney [3]. The domain is a rectangle $0 \le x \le 5$ microns and $0 \le y \le 2$ microns. In the 1D case (Test 1) we treat the entire 2 micron side at $x = 0$ as the surface exposed to the ambient gas, and in the 2D case (Test 2) we consider the regions along $x = 0$ where $0 \le y \le 0.5$ or $1.5 \le y \le 2$ as the exposed surface (see Fig. 1).

Figure 2 compares the behavior of different integration schemes for Test1 over a 60 second simulation time using a 25×5 mesh with a band solver. The step-size is automatically controlled to satisfy a user-specified error tolerance. The CPU timings for this simulation on a Cray J90 are as follows: 583 sec. for the backward Euler (order=1), 444 sec. for the 2nd order RKSI, 269 sec. for the 3rd order RKSI.

As we observe in this figure, the time-step increases by $5 - 6$ orders of magnitude within the first 60 seconds of

the simulation. (This trend continues as we integrate further into the time domain.) Numerical experiments using the iterative solvers demonstrate their increasing instability as the time-step increases. Since the matrix in the linear algebraic systems has the form $[\boldsymbol{I} - \Delta t \boldsymbol{A}]$ (with $\boldsymbol{I}$ being the identity matrix), the nonsymmetry and lack of diagonal-dominance of the Jacobian matrix $\boldsymbol{A}$ have a greater impact as Δt increases. Our numerical algorithm is implemented to optimize efficiency by using iterative methods for solving the linear systems whenever possible, and automatically reverting to a band solver if divergence is detected. We monitor the effectiveness of iterative schemes by keeping track of how frequently the band solver is called. Our experience showed that none of the iterative methods is effective after Δt increases above approximately 0.05, as the band solver is invoked for solving well over 50 % of the systems. For values of Δt below this, the most effective among the iterative methods we tested was CGSTAB, followed by the standard BCG and CGS schemes. Other methods that also worked satisfactorily in this range include a simplified 3-term QMR algorithm and the GMRES scheme. Methods that performed poorly included the Lanczos Orthores algorithm and the truncated Orthomin method.

The multigrid schemes performed somewhat better than the gradient iterative methods. With collective point Gauss-Seidel smoothing, the method remained effective up to about twice the time-step at which the iterative methods breakdown. We then switched to the line Gauss-Seidel forms, and found that with alternating line relaxation the multigrid method worked well up to $\Delta t \sim 0.25$, which is more than an order of magnitude better than the value for the iterative methods. This suggests that to improve performance further we need even better smoothing strategies.

Figures 3 and 4 show the computed solution for Test 1 using the 3rd order scheme after 60 and 600 seconds respectively. Figure 5 shows the phosphorus profile for the 2D case computed using a 25×25 mesh. Our multigrid studies showed that the relatively simple point smoothers are inadequate for solving most of the algebraic systems that are generated during a full simulation. With alternating line/block smoothers the behavior is better, but is still not robust enough as the time steps get larger. More work is needed to construct better multigrid smoothers.

V. Concluding Remarks

We have explored numerical integration, iterative solution and multigrid strategies for phosphorus diffusion modeling. Our investigations with semi-implicit Runge-Kutta integration methods suggest that the high-order forms of these schemes are promising for improving numerical performance. However, it is also important to develop efficient methods for solving the resulting algebraic systems, which are nonsymmetric and far from diagonal-dominance as the integration step sizes increase. In essence, what we have seen is that improving the integration methods leads to algebraic systems that are more

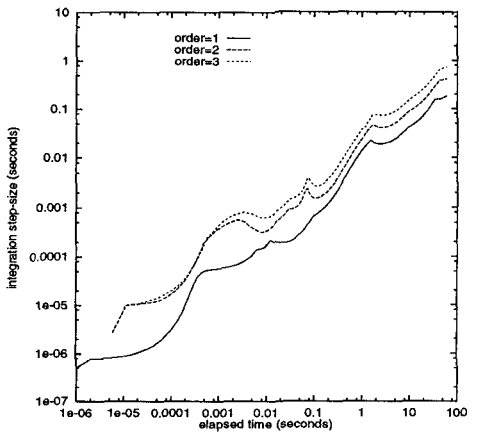

Fig. 2. Step-sizes of various integration schemes for a 60 second simulation of Test1.

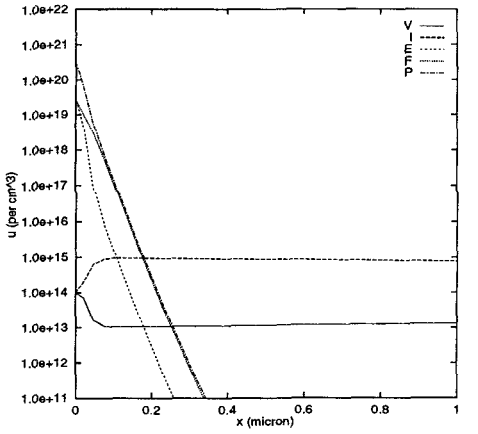

Fig. 3. Computed solution for Test1 after 60 seconds.

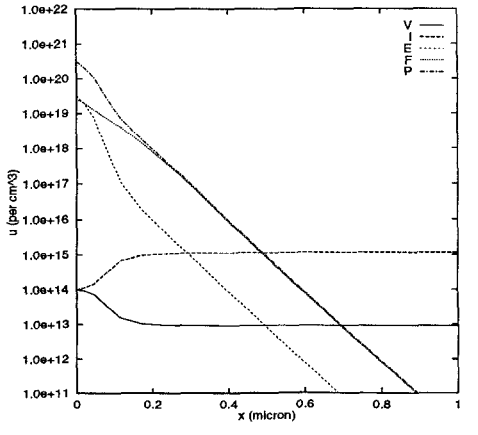

Fig. 4. Computed solution for Test1 after 600 seconds.

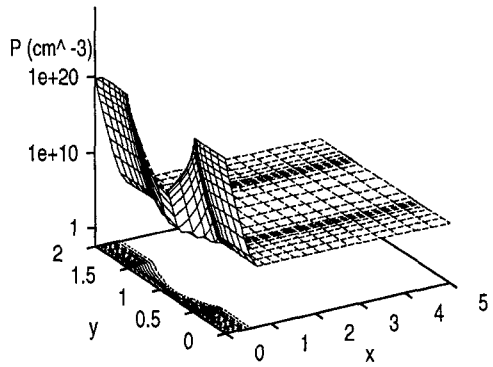

Fig. 5. Computed phosphorus profile for 2D test case after 60 seconds.

challenging to solve iteratively. Studies with generalized gradient iterative schemes demonstrate the difficulties in solving these systems. In order to improve the robustness of these iterative methods it appears necessary to construct better preconditioning and block-partitioning strategies. Multigrid methods performed better than the gradient iterative schemes. Our studies show that the use of better smoothing strategies increases the robustness of the multigrid algorithm, and permits much larger integration step-sizes. Investigation of new preconditioners and multigrid smoothing mechanisms is part of our ongoing work in this area.

ACKNOWLEDGMENTS

We wish to thank Walter Richardson, Bob Dutton and Conor Rafferty for helpful discussions.

REFERENCES

[1] H. R. Yeager and R. W. Dutton "An approach to solving multiparticle diffusion exhibiting stiff nonlinear coupling," *IEEE Trans. Electron Devices,* 32, 1964(1985).

[2] W. B. Richardson, G. F. Carey, and B. J. Mulvaney, "Modeling Phosphorus Diffusion in Three Dimensions", *IEEE Trans. on CAD,* 8, 487(1992).

[3] W. B. Richardson and B. J. Mulvaney, "Nonequilibrium behavior of charged point defects during phosphorus diffusion in silicon," *J. Appl. Phys.* 65, 2243(1989).

[4] L. Lapidus and J. H. Seinfeld, *Numerical Solution of Ordinary Differential Equations,* Academic press, New York, 1971.

[5] G. F. Carey, W. D. Joubert, H. Kohli, A. A. Lorber, R. T. McLay and Y. Shen, *PCG Programmer's Manual,* Report CNA-274, Center for Numerical Analysis, The University of Texas, Austin, 1995.

[6] P. Wesseling, *An Introduction to Multigrid Methods,* John Wiley, Chichester (England), 1992.